Hindawi
Geofluids
Volume 2021, Article ID 9994477, 15 pages
https://doi.org/10.1155/2021/9994477

Research Article

Investigation on Dewatering of a Deep Shaft in Strong Permeable Sandy Pebble Strata on the Bank of the Yellow River

Yuchao Zheng[1], **Jianyong Lei**[1], **Fei Wang**[2], **Liang Xiang**[2], **Jianfeng Yang**[1], **and Qingshuai Xue**[3]

[1]*Key Laboratory of Transportation Tunnel Engineering, Ministry of Education, School of Civil Engineering, Southwest Jiaotong University, Chengdu 610031, China*
[2]*China Railway First Survey and Design Institute Group Co., Ltd., Xian 710043, China*
[3]*Shenyang Qipeng Group Co., Ltd., Shenyang 110027, China*

Correspondence should be addressed to Yuchao Zheng; zhengyc218@126.com

Received 6 March 2021; Revised 17 August 2021; Accepted 29 August 2021; Published 24 September 2021

Academic Editor: Yi Xue

This paper reports the dewatering scheme of a deep excavation in sandy pebble strata. The excavation is in high permeability strata and is close to the Yellow River, making the dewatering difficult during construction. At present, few researchers have specially studied the dewatering scheme of deep excavations in strong permeable strata near the water resource. Field pumping test was conducted before the excavation activity, and the permeability coefficient of the strata was obtained by reverse analysis. According to the characteristics of the project, the dewatering scheme of "waterproof curtain + base grouting + pumping" was proposed. The influence of vertical waterproof curtain and base grouting on dewatering was analyzed by numerical simulation. In the construction process, the field water table and ground settlement were measured. The results show that (1) the groundwater table versus permeability coefficient curve shows three different stages and (2) the dewatering scheme of "waterproof curtain + base grouting + pumping" is effective for deep excavation in strong permeable strata.

1. Introduction

Many deep excavations or ventilation shafts have been designed and constructed in the rail transit projects, power tunnels, and water conveyance tunnels [1–3]. The construction of excavation pits below the groundwater table needs to lower the water table below the excavation face, so the dewatering scheme is vital. Effective dewatering measures are aimed at preventing uplift and fail of the base, avoiding quicksand and piping, and improving the stability and keeping the excavation face dry [4]. However, the dewatering work will lead to ground settlement inevitably. An ideal situation is to obtain the required drawdown with the least volume of pumped water to reduce the adverse impact on the surrounding environment [5, 6].

There are two common dewatering methods for excavation pits, one only uses pumping well and the other method is the cowork of pumping well and waterproof curtain. The pumping well method pumps out a large amount of groundwater, which forms a large cone of depression. The surrounding ground settlement will also be serious, which will damage the safety of adjacent buildings if any. Therefore, the combination of pumping well and waterproof curtain is widely used because of its less impact on the environment. For the excavation pit, because the diaphragm wall can be used as both a supporting structure and a good waterproof curtain, the cowork of waterproof curtain and pumping well is used for dewatering frequently [7–9].

Many researchers have studied on dewatering of deep excavations. Liu et al. [10] proposed inflow prediction formulas for excavation pits with partial penetrating curtains in high-permeability aquifers. Other researchers [11–13] focused on the deformation mechanism of diaphragm wall and ground settlement induced by dewatering. Zeng et al.

[14] and Zeng et al. [15] investigated ground settlement caused by preexcavation dewatering.

In excavation pit dewatering, in addition to pumping well and diaphragm wall, horizontal barriers have also been used. The base grouting was carried out for the excavation pit dewatering of Fuzhou Metro Line 2 [16], China, but there was no further analysis on base grouting. Granata and Leoni [17] reported a case that designed a grout blanket in order to decrease the water inflow from the bottom of the excavation, and the work focused mainly on the grouting activity quality control. It can be seen from the above practices that placing horizontal barriers is conducive to dewatering work when excavation under complex geological conditions.

In the past, it was rare to encounter an excavation pit with all the flowing three characteristics including a large excavation depth, a short distance from river, and high permeability sandy pebble strata. However, during the dewatering of the ventilation shaft between Lanzhou City University Station and South Shen'an Bridge Station of Lanzhou Metro Line 1, Gansu Provence, China, it encountered all these three characteristics. The depth of the shaft reaches 45.1 m, and the horizontal distance between the Yellow River embankment and the shaft center is only 105 m.

Both numerical simulation method and field observation were adopted in this paper. The influence of base grouting and waterproof curtain on dewatering was analyzed by numerical simulation. Then, the proposed dewatering scheme of "waterproof curtain + base grouting + pumping" was simulated. Field groundwater table and ground settlement were measured, and assembled data verified the results of the numerical simulation.

2. Project Background

2.1. Location of the Shaft. Lanzhou City is located on the floodplain of the upper reaches of the Yellow River. The shield tunnel of Lanzhou Metro Line 1 was bored underneath the bed of the Yellow River for about 317 m between Lanzhou City University Station and South Shen'an Bridge Station. A ventilation shaft was necessary in the north bank of the Yellow River for shield machine receiving and ventilation. Considering the depth of the tunnel and site conditions, the depth of the shaft reaches 45.1 m, and the horizontal distance between the Yellow River embankment and the shaft center is only 105 m. The location of the shaft is shown in Figure 1.

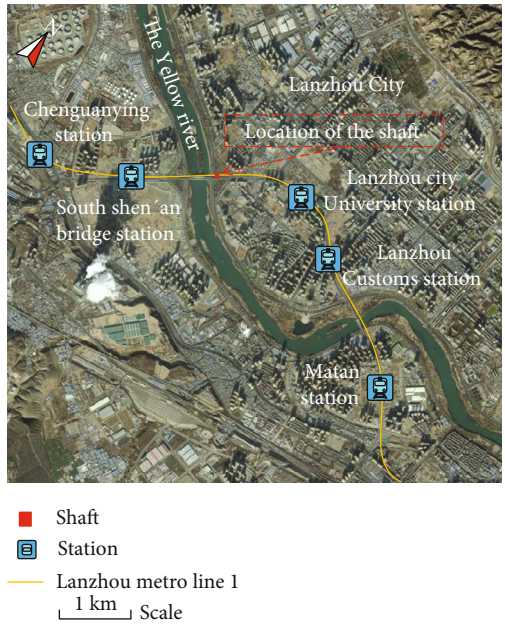

Figure 1: Location of the shaft.

2.2. Geology and Hydrogeology

2.2.1. Geology Conditions. Geological and hydrological conditions play a decisive role in the design of dewatering scheme. The geotechnical engineering investigation showed that the local strata were Quaternary, including 1-1 miscellaneous fill, 2-1 loess soil, 2-6 medium sand, 2-10 pebble, and 3-11 pebble, as shown in Figure 2. Medium sand was only sporadically distributed. The thickness of pebble 2-10 ranged from 5.7 m to 15.5 m, and that of pebble 3-10 was 200 m to 300 m. Consequently, 2-10 pebble and 3-11 pebble were mainly considered in this project for their large thicknesses.

A series of field tests (e.g., pumping test, field shear test, see Figure 3, and dynamic penetration test) and laboratory tests (e.g., grain size analysis and shear test) were carried out. The uniformity coefficient (C_u) of 2-10 pebble and 3-11 pebble is 159.04 and 19.34, respectively, and the coefficient of curvature (C_c) is 131.67 and 14.64, respectively. The grain size larger than 20 mm accounted for 63.5% of 2-10 pebble, and that value of 3-11 pebble is 64.53%. Figure 4 shows the 3-11 pebble layer. The suggested property parameters of the strata are shown in Table 1.

2.2.2. Hydrogeology. Groundwater mainly occurred in 2-10 pebble stratum and 3-11 pebble stratum, belonging to phreatic water with a water table of about -9.6 m, which was slightly higher than the water table of the Yellow River. The hydraulic connection between aquifer 2-10 and aquifer 3-11 was good. No confined water was found.

Two groups of single-well field pumping test were carried out to obtain the hydrogeology parameters. In each group, pumping tests of large drawdown, medium drawdown, and small drawdown were carried out. Four wells with the same diameter and depth were arranged in each group, one well served as pumping well, and the other three served as observation wells. According to field pumping tests, composition analysis of the aquifers, and regional engineering experience, the average permeability coefficient of each stratum was determined roughly, as shown in Table 1.

The permeability coefficient of anisotropic geotechnical medium is difficult to obtain directly, especially in complex geological conditions. The field pumping tests combined with inverse analysis can overcome the problem [5, 8, 18, 19]. Group-well pumping tests were carried out in the shaft, and an inverse analysis for hydrological parameters was carried out by Visual Modflow, a three-dimensional finite difference groundwater flow model software.

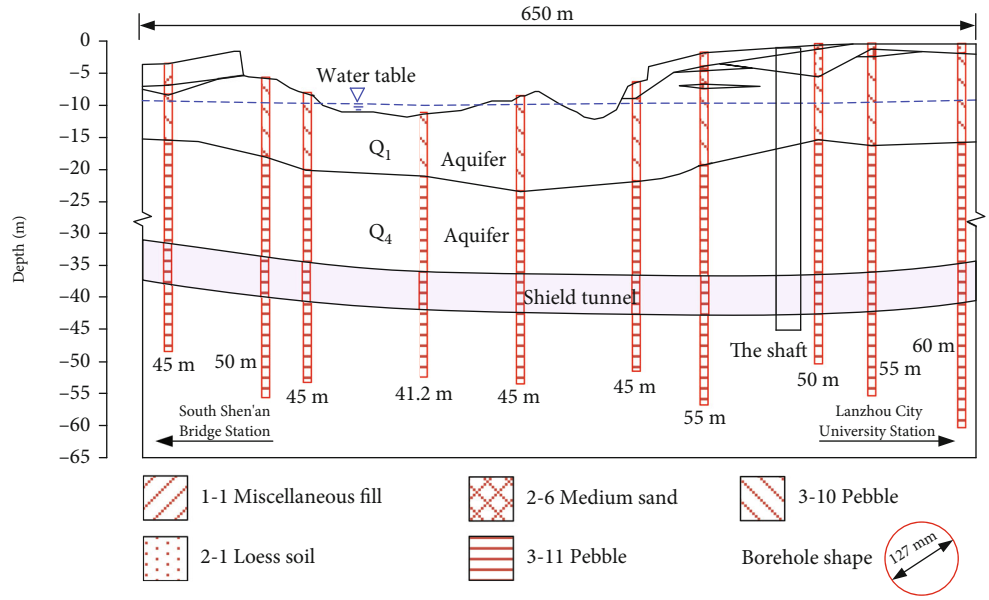

Figure 2: Longitudinal stratigraphic section.

Figure 3: Field shear test.

Figure 4: 3-11 pebble.

The permeability coefficients of 2-10 pebble and 3-11 pebble are shown in Table 2. It indicates that the horizontal permeability coefficient (K_H) is larger than the vertical permeability coefficient (K_V).

2.3. The Challenges. To summarize, the construction of the shaft presented several characteristics, including high permeability of aquifers, a large depth, and a short distance from the Yellow River. It brought several challenges:

(1) Dewatering was difficult. Due to the high permeability coefficient and strong seepage, it is uncertain that the water level can be reduced to the safe level only by the pumping well and vertical waterproof curtain

(2) In the thick and sandy pebble strata, the diaphragm wall is prone to defects which lead to leakage

(3) Construction safety risk is high. Due to the high water table and strong permeable aquifers, water table inside the pit will rise rapidly once the dewatering system fails, resulting in serious consequences

2.4. Preliminary Dewatering Scheme

2.4.1. Barrier Effect of Waterproof Curtain. The diaphragm wall is widely used for dewatering. In thick aquifer, diaphragm wall cannot penetrate to the aquitard [8]. Therefore, groundwater flows into the excavation pit through the bottom of the diaphragm wall [8, 11, 20]. The principle of diaphragm wall that can be used for dewatering is its barrier effect on seepage. It changes the seepage direction and seepage path of groundwater [21, 22].

(1) Seepage direction: the underground water flows into the pumping well horizontally without a barrier such as diaphragm wall. When pumping is conducted in cases with a barrier, the groundwater flow is three dimensional, both horizontal seepage and vertical seepage exist simultaneously [21, 22]. The vertical seepage consumes more energy and produces larger drawdown than the horizontal one for the vertical hydraulic conductivity is smaller than the horizontal conductivity [8]

Table 1: Strata property parameters.

Strata	Cohesion c (kPa)	Friction angle φ (°)	Density ρ (g/cm^3)	Void ratio e	Deformation modulus E_0 (MPa)	Permeability coefficient k (×10^{-4}m/s)
1-1 miscellaneous fill	0	12	1.71	—	5	0.58~0.93
2-1 loess soil	19	24.7	1.66	0.84	—	0.35~0.58
2-6 medium sand	0	30.0	1.90	—	12	2.3~2.90
2-10 pebble	0	35.0	2.17	0.282	45	6.60~7.41
3-11 pebble	15	43.0	2.28	0.288	50	5.79~6.37

Table 2: Inverse analysis results of permeability coefficient (×10^{-4} m/s).

Aquifers	Permeability coefficient	
	K_V	K_H
2-10 pebble layer	5.83	7.52
3-11 pebble layer	5.41	6.60

(2) Seepage path: the water outside the pit needs to bypass the bottom of the barrier to flow into the well in case of the existence of a barrier. It means that the barrier lengthens the seepage path so that the seepage time is also increased. In the initial stage of pumping, groundwater discharge mainly comes from inside the excavation pit. Groundwater head outside the pit begins to decline after a certain time because of the extension of the seepage path [21, 22]

2.4.2. Overview of the Shaft. The geometry of the shaft is rectangular in the plane with a size of 33.4 m × 20.4 m (see Figure 5), and the depth of the shaft was 45.1 m. The horizontal distance between the Yellow River embankment and the shaft center is only 105 m.

Given the wide use of diaphragm wall and pumping well, as well as some successful cases of base grouting, the dewatering scheme of "waterproof curtain + base grouting + pumping " was proposed.

Considering both dewatering design and excavation pit supporting design, the shaft was divided into 5 floors, named F1 to F5 from top to bottom, as shown in Figure 6. The shaft was composed of main structures (including side wall, floor slab, beam and column), the inner diaphragm wall (inner waterproof curtain) and the outer diaphragm wall (outer waterproof curtain) (see Figure 6). The main structures were made of reinforced concrete. The inner diaphragm wall was made of C40 (its Young's modulus $E = 34$ GPa) reinforced concrete with a thickness of 1.2 m and a depth of 60.1 m. The outer plain concrete diaphragm wall was 0.8 m thick and 51.1 m deep. Sleeve-valve-pipe grouting (base grouting) was implemented in a range of 10 m below the bottom to improve the strata properties.

In order to ensure safety of shield boring, side grouting reinforcement range was in the shield passing area between the outer waterproof curtain and the inner waterproof curtain at the depth of 32.15 m to 50.15 m, as shown in Figure 6.

The space was divided into three parts by the two waterproof curtains, as shown in Figure 5. The space inside the inner waterproof curtain was area I, the space between the inner waterproof curtain and outer waterproof curtain was area II, and the space outside the outer waterproof curtain was area III.

2.4.3. Drawdown Required. Limit equilibrium method assumes that water inrush does not occur when the gravity of the overlying soil is larger than the water pressure under a coefficient, expressed as [9, 23]

$$F = \frac{\gamma_s (H - h_s)}{\gamma_w (H - D)}, \quad (1)$$

where F is the safety factor, h_s is the excavation depth (m), D is the water head of confined aquifer (m), H is the depth of the confined aquifer roof (m), γ_s is the unit weight of soil between the excavation pit bottom and the confined aquifer roof, with a value of 21 kN/m^3 here, and γ_w is the unit weight of base grouting area, with a value of 25 kN/m^3 in this paper.

Formula (1) was used to obtain the safety water table required by 7 different excavation depths (excavation depth: 10 m, 20 m, 30 m, 31.2 m, 35 m, 40 m, and 45.1 m). The comparison of excavation depth and safe water table is as Table 3 at safety factor $F = 1.2$. The limit excavation depth of the shaft was 31.2 m. Therefore, when the excavation depth was less than 31.2 m, pumping inside the shaft prevailed to make the excavation face dry. When the excavation face was lower than -31.2 m, pumping wells inside and outside the shaft should work together.

2.4.4. Layout of Pumping Wells. It was preliminarily designed to arrange 9 pumping wells (W1 to W9, among which W5 was for observation, also represented by O1) in area I, 6 pumping wells (W10 to W15) in area II, and 52 pumping wells (W16 to W67, among which W47, W53, W59, and W65 were observation wells, also represented by O2 to O5, respectively) in area III. Figure 7 shows the layout of the pumping wells. Details of pumping wells are shown in Table 4. The depth of the wells in area I was 55 m with a diameter of 650 mm and a filter length of 15 m. The 6 wells in area II were 60 m deep and were steel pipe wells. Cement well with a depth of 60 m, a diameter of 800 mm, and a filter length of 30 m was adopted in area III.

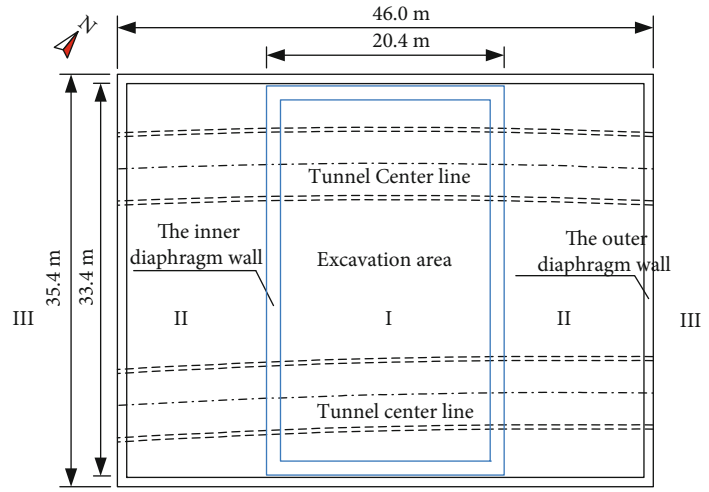

Figure 5: Top view of the shaft.

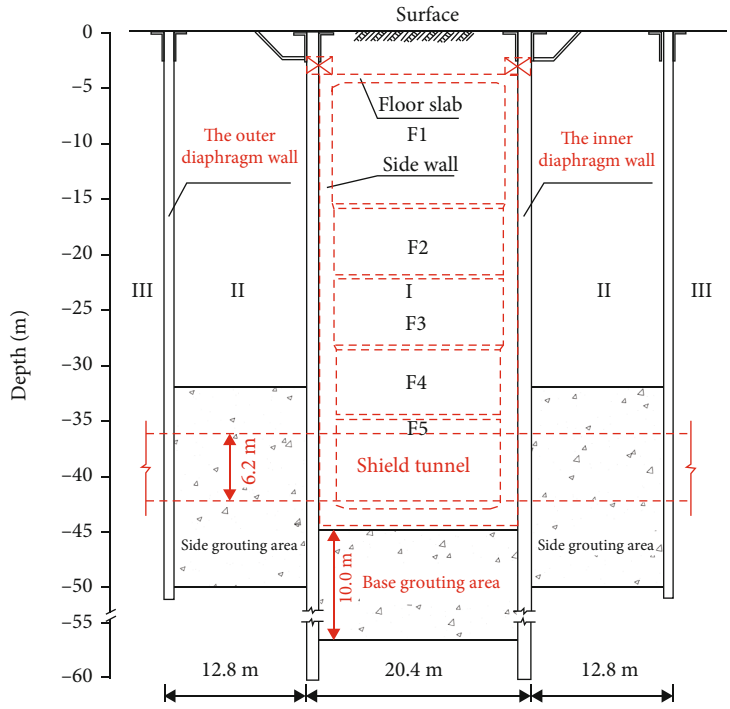

Figure 6: Section view of the shaft.

Table 3: Comparison of excavation depth and safe water table (m).

Excavation depth	Safe water table outside the shaft	Drawdown required
10	-10	0
20	-10	0
30	-10	0
31.20 (critical excavation depth)	-10	0
35	-16.7	6.7
40	-25.4	15.4
45.1	-34.2	24.2

3. Numerical Simulation

The feasibility of the planned dewatering scheme needs to be examined. This section mainly focuses on three issues: (i) the influence of vertical waterproof curtain on dewatering, (ii) the influence of base grouting on dewatering, and (iii) the numerical simulation of the proposed dewatering scheme of "waterproof curtain + base grouting + pumping."

3.1. Mechanism of Seepage Analysis. Formula (2) [4, 9] is the governing equation of three-dimensional transient flow in anisotropic porous media. It is also the constitutive model used in this paper. In Visual Modflow, the numerical

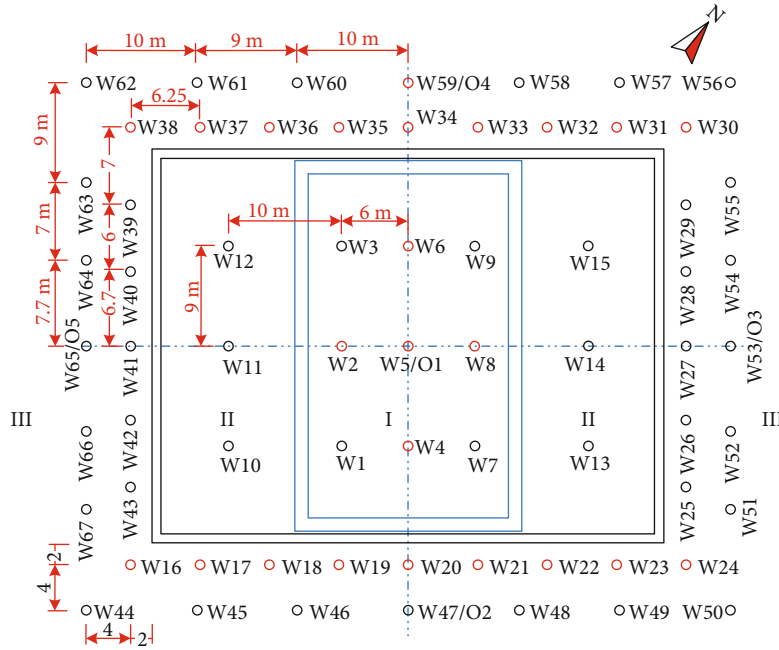

Figure 7: Layout of pumping wells (m).

Table 4: Details of pumping wells.

Well location	Quantity	Diameter (mm)	Filter length (m)	Depth of well (m)	Type of well
In area I	9	650	15	55	Steel pipe well
In area II	6	650	30	60	Steel pipe well
In area III	52	800	30	60	Cement well

simulation model can be obtained by discretizing the mathematical model with the finite difference method.

$$\begin{cases} \dfrac{\partial}{\partial x}\left(k_{xx}\dfrac{\partial h}{\partial x}\right)+\dfrac{\partial}{\partial y}\left(k_{yy}\dfrac{\partial h}{\partial y}\right)+\dfrac{\partial}{\partial z}\left(k_{zz}\dfrac{\partial h}{\partial z}\right)-W=S_s\dfrac{\partial h}{\partial t}, & (x,y,z)\in\Omega, \\ h(x,y,z,t)\big|_{\Gamma_1}=h_1(x,y,z), & (x,y,z)\in\Gamma_1, \\ k_{xx}\dfrac{\partial h}{\partial n_x}+k_{yy}\dfrac{\partial h}{\partial n_y}+k_{zz}\dfrac{\partial h}{\partial n_z}\Big|_{\Gamma_2}=q(x,y,z,t), & (x,y,z)\in\Gamma_2, \\ h(x,y,z,t)\big|_{t=t_0}=h_0(x,y,z), & (x,y,z)\in\Omega, \end{cases} \tag{2}$$

where k_{xx}, k_{yy}, and k_{zz} are the hydraulic conductivity in the x, y, and z directions (cm/s); h is the water table in position (x, y, z) (m); S_s is the specific storage rate in position (x, y, z) (m^{-1}); n_x, n_y, and n_z are the unit normal vectors on boundary Γ_2 along the x, y, and z directions, respectively; W is the recharge and discharge of the groundwater (d^{-1}); t is time (h); Γ_1, Γ_2 are the first and second types of boundary condition, respectively; q is the lateral recharge per unit area on boundary Γ_2 (m^3/d); $h_0(x, y, z)$ is the initial water table in position (x, y, z) (m); and Ω is the calculation domain.

3.2. Influence of Vertical Waterproof Curtain

3.2.1. Analysis Cases. Four analysis cases were set to analyze the influence of waterproof curtain on excavation pit dewatering, as shown in Table 5. There was no waterproof curtain

Table 5: Four analysis cases.

Case	Inner waterproof curtain	Outer waterproof curtain	Base grouting
1	×	×	×
2	√	×	×
3	√	√	×
4	√	√	√

Table 6: Parameters of aquifers in the model.

Aquifer	Specific storage S_s (1/m)	Specific yield S_y	Permeability coefficient (m/s)	
2-10 pebble	5.0×10^{-4}	0.2	K_V	5.83×10^{-4}
			K_H	7.54×10^{-4}
3-11 pebble	5.0×10^{-4}	0.2	K_V	5.41×10^{-4}
			K_H	6.60×10^{-4}

in case 1, the inner waterproof curtain was set in case 2, and the inner and outer waterproof curtains were set in case 3. From case 1 to case 3, all 67 pumping wells were on working. In case 4, both base grouting and the two waterproof curtains were set, the permeability coefficient of base grouting area was 1.0×10^{-7} m/s, and 52 pumping wells outside the pit and 3 in area I were turned on. Simulation time of each case was 10 days.

3.2.2. Three-Dimensional Seepage Model. Considering the influence range of dewatering, the size of the model was determined to be 1200 m × 1200 m, and the height was 150 m. In Visual Modflow, the analysis type was transient flow for this simulation.

The boundary condition was simulated by Constant Head package with the water table of -10.0 m. Using the River package to simulate the Yellow River, its water table was set at -10.0 m. The coordinate origin was situated at the center of the shaft surface. Waterproof curtain was simulated by Wall package with the permeability coefficient of 1.84×10^{-12} m/s (considering the antiseepage grade of P8). Pumping wells were simulated by the Well package. According to the results of the field pumping tests, the pumping rate of each well in area I and area II was set to 100 m^3/h while the pumping rate of each well in area III was 150 m^3/h. Aquifers of 2-10 pebble and 3-11 pebble were mainly considered in the model. Hydrological parameters of the aquifers were determined according to the results of the field pumping tests and inverse analysis, and the values used in the simulation are as shown in Table 6.

The model for case 4 is as shown in Figure 8, and Figure 9 presents the model of diaphragm wall and pumping wells. It was divided into 8 layers vertically. The horizontal mesh became sparse from the shaft center to outside, a total of 214 rows and 214 columns. The finite difference mesh had a total of 416025 nodes and 366368 elements.

3.2.3. Results. Figure 10 shows the cone curve of depression in each case. The cone curve of depression became steep near the Yellow River and relatively flat away from the Yellow River.

In case 1, the cone curve of depression was smooth, and water table in area I was reduced to -35.0 m. In case 2 to case 4, the water table in area I was -46.9 m, -51.0 m, and -53.3 m, respectively.

For the water table in area I: in case 1, the water table cannot be lowered to the bottom of the pit, and the water table in case 2 to case 4 was lower than the bottom of the pit. The drawdown in case 3 was 11.1% more than that in case 2. The drawdown in case 4 was 17.3% more than that in case 2. The drawdown in case 4 was 5.6% greater than that in case 3, although the number of pumping wells in case 4 was only 82.1% of that in case 3.

For the water table in area II: on the Yellow River side, the water table of case 1 to case 4 was -33.9 m, -29.2 m, -34.2 m, and -43.6 m, respectively. Obviously, neither case 1 nor case 2 can meet the safety requirement. Case 3 can just meet the requirement, and case 4 can meet the requirement. The drawdown of case 4 was 1.39 times than that of case 3.

The above analysis account for the cowork of base grouting and two vertical waterproof curtains forms a relatively impervious space and isolates the hydraulic connection of inside and outside the shaft.

3.3. Influence of Base Grouting

3.3.1. Analysis Cases. Grouting is an effective method to block water in underground engineering [24]. Grouting reinforcement of weak strata improves the mechanical properties (compression modulus, cohesion, friction angle, and permeability coefficient) of the reinforced area. Some mesotable studies such as literatures [25, 26] involved the diffusion mechanism of slurry and tried to simulate it by numerical method. However, the determination of parameters is complicated, and its applicability needs to be improved in practice.

In this paper, the grouting effect is considered from a macro perspective. Permeability coefficient is set in the base grouting area to reflect the reinforcement effect in simulation. In each analysis cases, the two waterproof curtains were set; the differences were the permeability coefficient of the base grouting area and the number of pumping wells in operation. For the permeability coefficient of the base grouting area, there were 10 different values (6×10^{-4} m/s, 4.5×10^{-4} m/s, 3.2×10^{-4} m/s, 2.2×10^{-4} m/s, 1.4×10^{-4} m/s, 8.5×10^{-5} m/s, 4.4×10^{-5} m/s, 1.9×10^{-5} m/s, 5.8×10^{-6} m/s, and 7.5×10^{-7} m/s). For pumping wells, all 52 wells in area III and all 6 wells in area II were in operation in each case, and the number of pumping wells in area I varied from 1 to 9. A total of 53 analysis cases were simulated. The simulation time was 30 days.

The constitutive model used was transient flow. The size of the model was 1200 m × 1200 m × 150 m. It was divided into 8 layers, 214 rows and 214 columns with a total of 416025 nodes and 366368 elements. The boundary condition of constant water head was simulated by Constant Head package with the water table of -10.0 m. The Yellow River

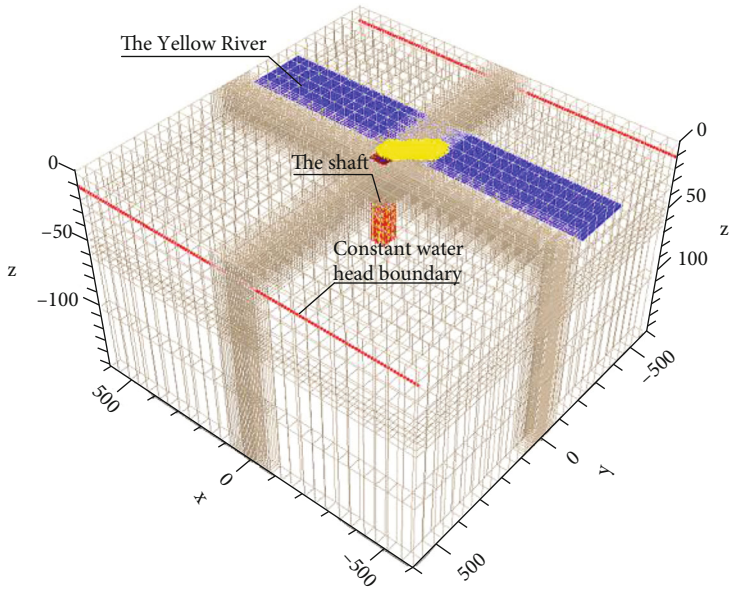

Figure 8: Mesh of three-dimensional model.

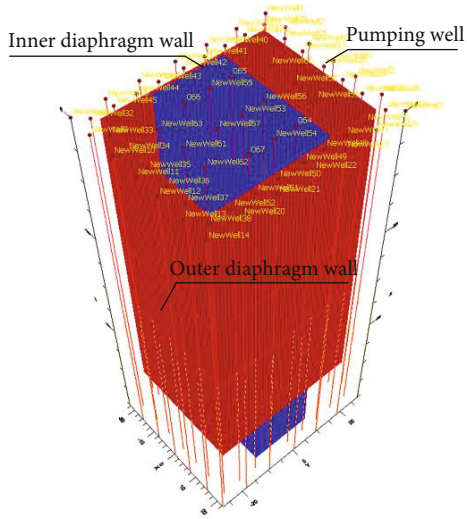

Figure 9: Model of diaphragm wall and pumping well.

was simulated by River package with the water table of -10.0 m. Waterproof curtain was simulated by Wall package with the permeability coefficient of 1.84×10^{-12} m/s. Pumping wells were simulated by the Well package. The pumping rate of each operative well in area I and area II was set to 100 m^3/h while in area III the pumping rate was 150 m^3/h. The pumping rate of the inoperative well was set to 0 m^3/h. Hydrological parameters of the aquifers are as shown in Table 6.

3.3.2. Result. The water table in area I is shown in Figure 11. From the perspective of slope, the groundwater table versus permeability coefficient curve shows three different stages.

Stage 1: when the permeability coefficient is greater than 1.4×10^{-4} m/s, the curve is almost a flat line. In this stage, with the decrease of permeability coefficient, the water table is slowly decreasing. According to different curves, the decline of water table in area I is mainly affected by the number of pumping wells in area I.

Stage 2: the curvature of curve changes rapidly. The permeability coefficient is between 1.9×10^{-5} m/s and 1.4×10^{-4} m/s in this stage. With the decrease of permeability coefficient, the decline rate of groundwater table accelerates.

Stage 3: the water table shows a linear downward trend with a large slop. When the permeability coefficient is less than 1.9×10^{-5} m/s, the water table decreases linearly with the decrease of permeability coefficient.

The dewatering results are closely related to the permeability coefficient of the grouting area. A large permeability coefficient does no obvious effect on dewatering. A small permeability coefficient significantly benefits the dewatering work while it is difficult to achieve. Therefore, the permeability coefficient of grouting area should be controlled in stage 3. For this project, the coefficient is recommended to be 1×10^{-7} m/s.

3.4. Simulation of Dewatering Scheme. In Sections 3.2 and 3.3, the effect of vertical waterproof curtain and base grouting on dewatering is analyzed, but the process of dewatering is not considered. According to the analysis in Section 2.4.3, the required drawdown is different under different excavation depths. Therefore, in the actual excavation process, the dewatering well should be turned on in several stages according to the excavation depth. In this part, the proposed dewatering scheme of "waterproof curtain + base grouting + pumping" is simulated.

3.4.1. Simulation Process. The simulation was carried out in 9 stages, shown in Table 7. The simulation process is as follows: in stage 1, pumping is not carried out because the groundwater table is about -10 m. In stage 2, turn on 2 wells in area I. In stage 3, turn on 4 wells in area I. Stage 4 is to

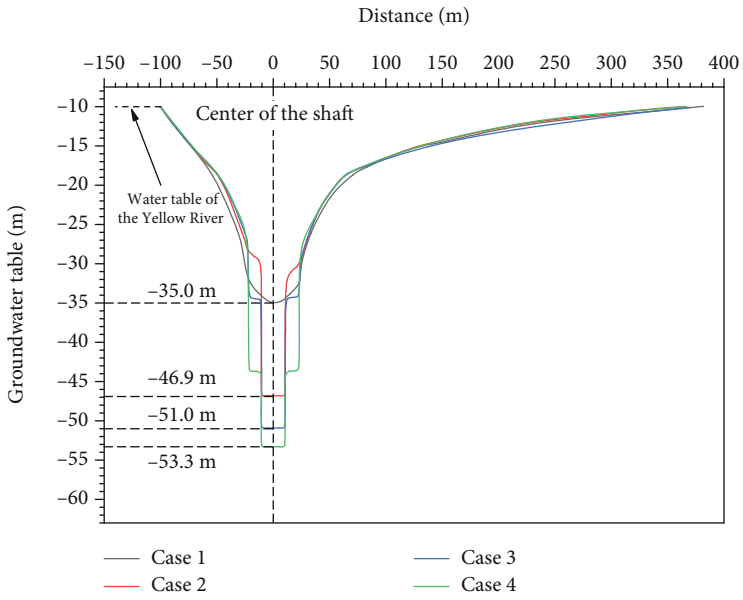

Figure 10: Cone curves of groundwater depression of the 4 analysis cases.

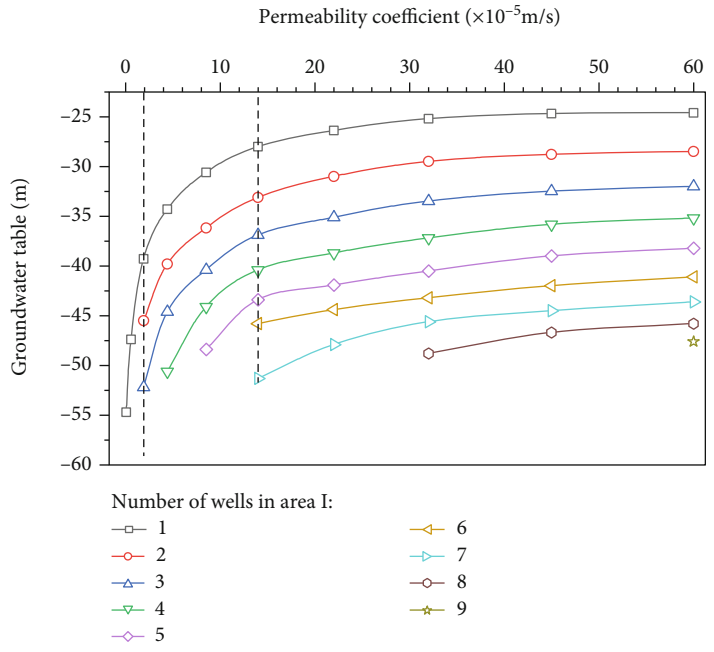

Figure 11: Water table of different analysis cases.

turn on 6 wells in area I. Thereafter, the permeability coefficient of the base grouting area is set to 1×10^{-7} m/s. Then, turn on 1 well in area I, 6 wells in area II, and 4 wells in area III to conduct the stage 5 analysis. In stage 6, the number of wells in area III is 12. In stage 7, the number of wells in area III is 20. In stage 8, 40 wells are in operation in area III. In stage 9, 52 wells are working in area III.

The constitutive model used was transient flow. The size of the model was 1200 m × 1200 m × 150 m which was divided into 8 layers, 214 rows and 214 columns with a total of 416025 nodes and 366368 elements. The boundary condition was simulated by Constant Head package with the water table of -10.0 m. The Yellow River was simulated by River package with the water table of -10.0 m. Waterproof curtains were simulated by Wall package with the permeability coefficient of 1.84×10^{-12} m/s. The pumping rate of each operative well in area I and area II was set to 100 m^3/h while in area III the pumping rate was 150 m^3/h. The pumping rate of the inoperative well was 0 m^3/h. Hydrological parameters of the aquifers are as shown in Table 6. The permeability coefficient of the base grouting area was 1×10^{-7} m/s.

Table 7: Operation scheme of pumping wells.

Stage	Number of pumping wells			Water table (m)		Excavation depth (m)	Description
	Area I	Area II	Area III	Area I	Area II		
1	—	—	—	-10.0	-10.0	0.00~10.00	Excavation of F1
2	2	—	—	-18.4	-10.0	10.00~17.68	
3	4	—	—	-25.6	-10.0	17.68~24.08	Excavation of F2
4	6	—	—	-32.5	-10.0	24.08~30.48	Excavation of F3
Grouting the base during the excavation of F3 with the target permeability coefficient of 1×10^{-7} m/s							
5	1	6	4	-54.2	-17.4	30.48~35.50	Excavation of F4
6	1	6	12	-54.2	-20.1	35.50~36.78	
7	1	6	24	-54.4	-24.1	36.78~39.00	
8	1	6	40	-54.8	-28.8	39.00~42.00	Excavation of F5
9	1	6	52	-54.8	-34.2	42.00~45.10	

3.4.2. Result. The water table of different stages is shown in Table 7. From stage 1 to stage 4, there was no grouting at the base, and the pumping wells in the area I varied from 0 to 6. The water table in area I dropped from -10.0 m to -32.5 m while the water table in area II changed little. It shows that the pumping well in area I cannot effectively lower the water table in area II when there is no grouting at the base. Since the critical excavation depth is 31.2 m, the purpose of pumping is to reduce the water table in area I to ensure the dryness of the excavation face. According to the water table of simulation results, the excavation depth of each stage can be obtained. And F1 to F3 can be excavated during stage 1 to stage 4, shown in Table 7.

After the base grouting, the water table in area I maintained between -54.2 m and -54.8 m from stage 5 to stage 9. As the number of pumping wells in area III increased from 4 to 52, the water table in area I changed little, while the water table in area II decreased from -17.4 m to -34.2 m. After the base grouting was completed, a horizontal waterproof curtain was formed. Only one pumping well was needed inside the pit to keep the water table below -54.2 m. The decrease of water table in area II was mainly due to the increase of the number of wells in area III. According to the water table inside the pit and outside the pit, F4 and F5 can be excavated during stage 5 to stage 9, as shown in Table 7.

4. Field Observation

The dewatering scheme of "diaphragm wall + base grouting + pumping" was used, and the ventilation shaft was accomplished. Field observation data were validated against the simulation results to verify the reliability of the three-dimensional model.

4.1. Field Dewatering

4.1.1. Excavation Strategies. The results of numerical simulation indicated that the preliminary designed dewatering scheme of "diaphragm wall + base grouting + pumping" was effective. And it was used in the construction of the shaft. The overview of the shaft is provided in Section 2.4.2. Figure 7 shows the layout of the pumping wells.

The shaft was constructed by reversed construction method. It was excavated in layers using mechanics. Firstly, the inner diaphragm wall and the outer waterproof curtain were constructed, and the sleeve-valve-pipe grouting method was used for side grouting. Secondly, preexcavation pumping test was conducted to check the reliability of the dewatering scheme and the quality of the diaphragm wall. Thirdly, it constructed the capping beam of the inner diaphragm wall and the horizontal reinforced concrete strut beam at the top of the main structure. Then, the shaft was excavated from F1 to F5 one after another; the construction sequence of each floor was excavating to bottom of each floor, applying horizontal strut beam, and concreting the side wall of the same floor. During the excavation of F3 layer, base grouting was carried out, and the target permeability coefficient was 1.0×10^{-7} m/s. After receiving of the shield machine, the construction of the floor slab was conducted from F5 to F1. Finally, the ground was restored.

In excavation engineering, it is generally necessary to lower the water table to 0.5 m below the excavation face. Therefore, this paper took the water table 0.5 m below the excavation face as the water table control criterion.

In order to reduce the impact of dewatering on the environment, the staged dewatering strategy was implemented according to different excavation depths referring to the excavation stages in Table 7. During the excavation of the initial 10 m, no pumping well was required. During the excavation of the remaining part of F1, turn on 2 wells in area I. With the deepening of excavation, the number of pumping wells was gradually increased according to the actual situation of the site.

4.1.2. Preexcavation Pumping Test. The preexcavation pumping test is an effective method to check the reliability of the dewatering scheme and the quality of the diaphragm wall [27]. Therefore, the preexcavation pumping test was conducted after the construction of diaphragm wall.

Only 5 pumping wells were constructed in area I and 19 in area III for the preexcavation pumping test (each well was marked in red in Figure 7, and among which W5, W24,

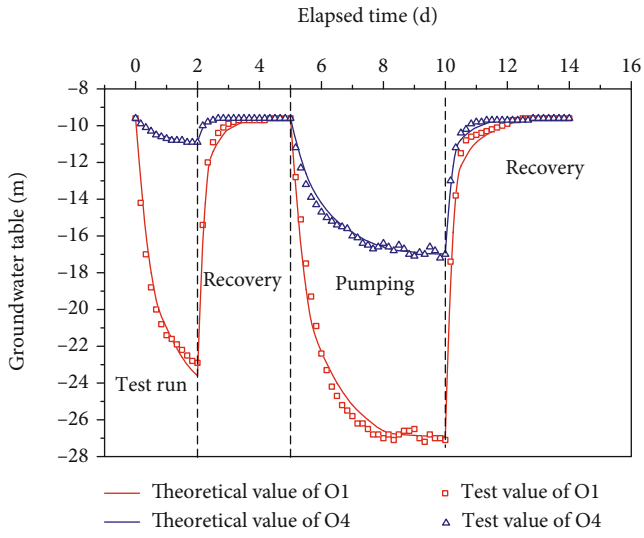

Figure 12: Water table of preexcavation pumping test and inverse analysis.

W38, and W59 were used as observation wells). During the pumping test, 4 pumping wells in area I were in operation for trial operation for 2 days, and then, all 20 pumping wells were turned on. The pumping was stopped after the water table of the observation wells was stable. The measured groundwater table of wells O1 and O4 is as shown in Figure 12.

Inverse analysis was carried out by Visual Modflow based on preexcavation pumping test results, and the inverse analysis results of well O1 and well O4 are as shown in Figure 12. The permeability coefficients of aquifer 2-10 and aquifer 3-11 were obtained accurately. Vertical permeability coefficient (K_V) and horizontal permeability coefficient (K_H) of aquifer 2-11 were 5.65×10^{-4} m/s and 7.15×10^{-4} m/s, respectively. For aquifer 3-11, K_V was 5.34×10^{-4} m/s and K_H was 6.34×10^{-4} m/s. Given the diaphragm wall had been completed before the preexcavation test, the effect of diaphragm wall was also taken into consideration in the inverse analysis. The existence of the diaphragm wall made the results of the two inverse analysis (the other inverse analysis is in Section 2.2) different with the maximum difference of 4.92%. It can be explained that the parameters used in the modeling were precise enough. The pumping tests verified the quality of the diaphragm wall was good.

4.1.3. Grouting Parameters. The grouting will directly affect the dewatering results. Splitting grouting method was adopted for the base grouting. PVC sleeve-valve-pipe with a diameter of 65 mm was used. The grouting boreholes were arranged with equilateral triangles with a spacing of 1.2 m. The target diffusion radius of each grouting hole was 0.8 m, as shown in Figure 13. The grouting material of the upper 3 m of the base grouting area was ordinary Portland cement, and the water-cement ratio was controlled between 0.8 : 1 and 1 : 1. The grouting material of the lower 7 m was mixed slurry made of ordinary Portland cement and sodium silicate with a volume ratio of 1 : 0.8. The grouting pressure was 2 to 3 MPa.

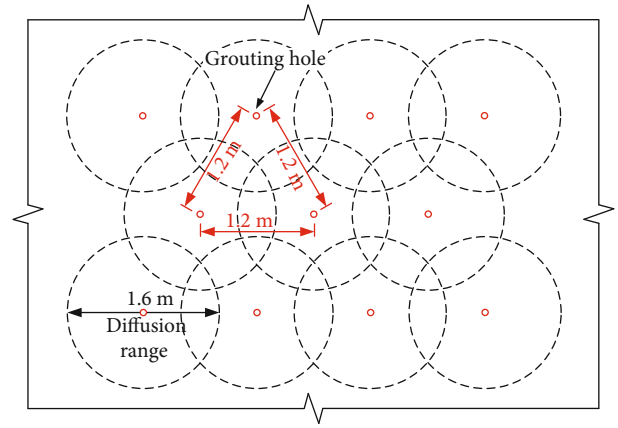

Figure 13: Layout of grouting hole and slurry diffusion.

4.2. Water Table Observation. The observation of the groundwater table (observation points WT1 to WT7 are shown in Figure 14) began from June 26, 2015, to April 24, 2016, lasting for 304 days [2]. Groundwater table versus time curve is plotted, such as shown in Figure 15.

Starting from June 26, 2015, all pumping wells were put into trial operation for 13 days. From the 13th day to the 97th day, F1 and F2 were excavated. At this stage, according to the excavation progress, the pumping wells in area I were turned on step by step to ensure the water table in the pit was below the excavation face beyond 0.5 m. The drawdown in area II and area III was very weak, and the water table difference of each observation well (WT1 to WT6) was very small. It can be interpreted that the groundwater discharge mainly comes from inside the excavation pit in this stage.

During the excavation of F3, in order to prevent inrush, some wells outside the pit were turned on, and the water table of observation wells WT1 to WT4 dropped to -15 m. Water table in area II changed about 2.7 m. Water table in area I dropped to about -36.2 m.

From the 138th day to the 230th day, F4 and F5 were excavated. During this time, all 6 wells in area II were in operation and the number of pumping wells in area III was gradually increased in several stages. As a result, the water table in area III gradually reduced to -36 m while the water table in area II rapidly dropped to about -35 m. The water table in area I was -46.1 m. After the bottom of the shaft was constructed, the number of pumping wells reduced in two stages until the water table returned to normal table. Moreover, during the construction, no obvious leakage was found in the waterproof curtain.

4.3. Ground Settlement Observation. The measurement of ground settlement began from June 26, 2015, lasting for 340 days. The observation points are shown in Figure 14. The settlement versus time curve is shown in Figure 16.

It can be seen from Figure 16 that ground settlement is closely related to dewatering process. In the construction run, the maximum settlement was -6.56 cm, which was acceptable.

Most of the settlement occurred in the 1st day to the 138th day, that was, during the excavation of F1 to F3. According to GS09-5, the settlement occurred during the

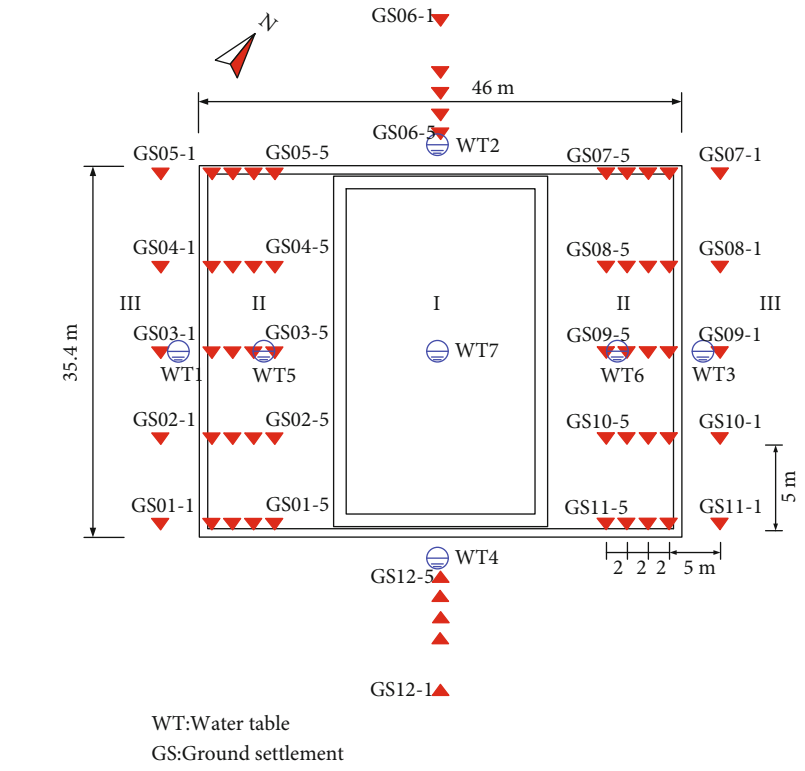

Figure 14: Layout of observation points for underground water table (WT) and ground settlement (GS). (The numbers of the 2nd to the 4th observation points on each observation section are not marked.)

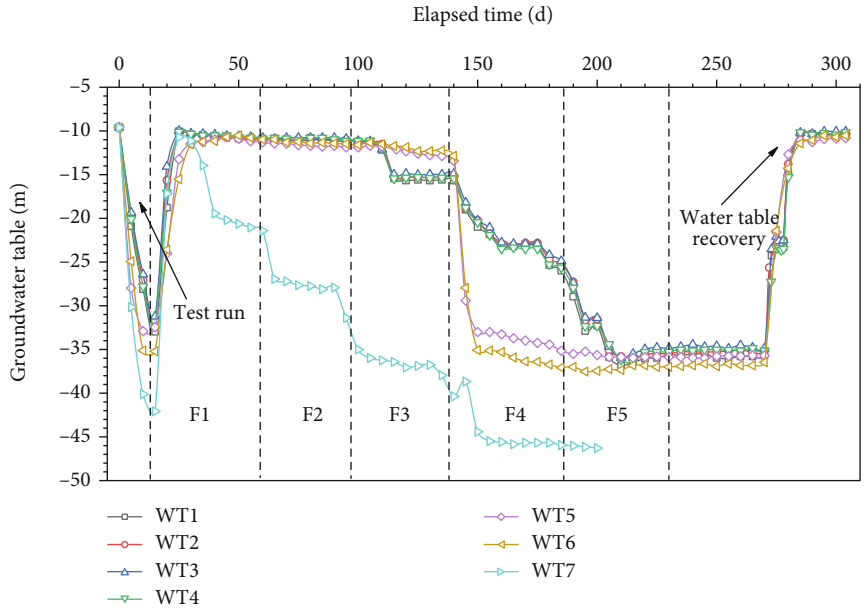

Figure 15: Observation results of underground water table.

excavation of F1 to F3 which accounts for 88.4% of the maximum settlement. There may be two reasons for this. First, the upper structures were not stable during this time; the effect of dewatering and excavation unloading together leads to large ground settlement. Second, the base was grouted during the excavation of F3, and the upper structure was gradually stable. The base grouting area, the diaphragm wall, and the horizontal strut beam formed a combined support system, and the structural stiffness increased, which led to the following excavation cause small settlement.

During the excavation of F4 to F5, the ground settlement gradually stabilized. After concreting the bottom of the shaft,

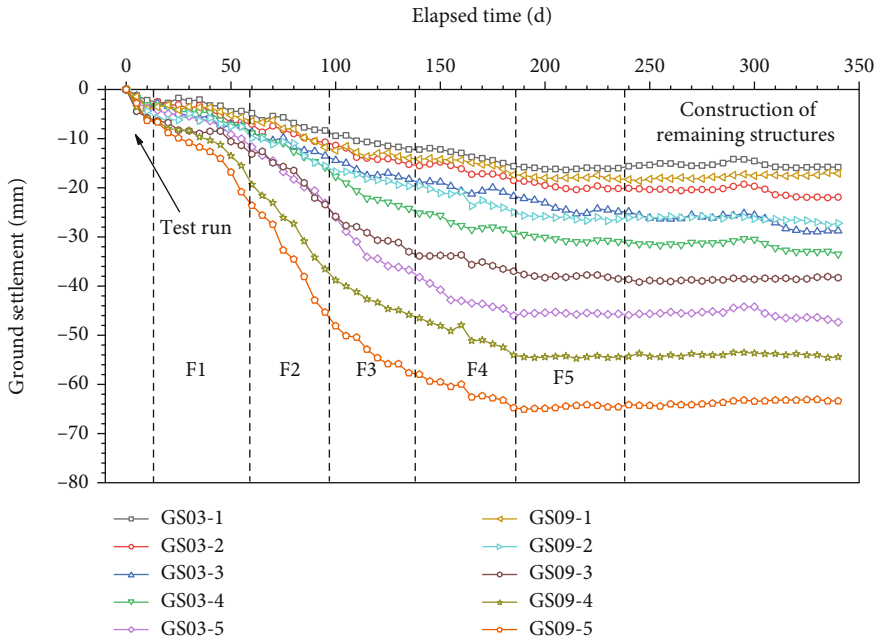

Figure 16: Ground settlement curve.

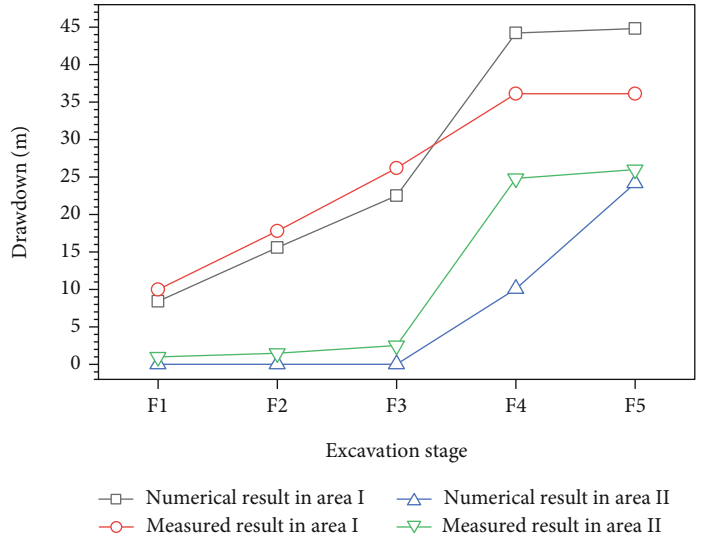

Figure 17: Comparison of drawdown.

the ground settlement raised slightly due to the recovery of groundwater table.

5. Validation

Since the ground settlement is not considered in the numerical simulation, the main parameter for validation is the groundwater table. The measured water table is compared with the numerical results of Section 3.4.2, as shown in Figure 17.

During the excavation of F1, the drawdown obtained by numerical simulation was 8.4 m and the measured drawdown was about 10 m in area I, which indicated that the simulation result is 16% smaller than the measured result. The simulated result of drawdown in area I was 12.3% lower than the measured one during the excavation of F2.

During the excavation of F3, the water table in area II decreased to -12.5 m, which was 2.5 m deeper than the simulation result. The simulated result of drawdown in area I was 14.1% smaller than the measured result.

During the excavation of F4, the water table in area I was -46.1 m, while the numerical result was -54.2 m. The water table in area II was -35 m, while the simulated result was -20.1 m.

During the excavation of F5, the drawdown in area I was 36.1 m, while the numerical result was 44.8 m. The measured drawdown in area II was about 26 m, while the simulated result was 24.2 m, and the difference was only 6.9%.

To summarize, the measured results are in good agreement with the numerical results during the excavation of F1 to F3 and F5. The difference is mainly reflected in the excavation of F4. This is because in order to ensure the safety of the project, the pumping wells in area III was increased during the excavation of F4. Therefore, the numerical simulation is reliable.

6. Conclusions

In this paper, the method of numerical simulation was adopted to analyze the dewatering scheme. The project was successfully implemented, which verified the reliability of the dewatering analysis. The following conclusions are obtained:

(1) The groundwater table versus permeability coefficient curve shows three different stages. The permeability coefficient of grouting area is recommended to be controlled in stage 3. For this project, the recommended value is 1×10^{-7} m/s

(2) The design of the inner waterproof curtain and outer waterproof curtain leads to a large drawdown. When two waterproof curtains are used, the drawdown is 11.1% larger than that in case with one waterproof curtain

(3) The dewatering scheme of "waterproof curtain + base grouting + pumping" is effective for deep excavation in strong permeable strata

Data Availability

The data used to support the findings of this study are available from the corresponding author upon request.

Conflicts of Interest

The authors declare that there is no conflict of interest regarding the publication of this paper.

Acknowledgments

The authors would like to thank the financial support from China Railway First Survey and Design Institute Group Co., Ltd. and Lanzhou Rail Transit Co., Ltd. (Grant No. 13-17). Thanks are due to the China Railway First Survey and Design Institute Group Co., Ltd. and the China Railway No.14 Engineering Group Co., Ltd. for providing great assistance in field water table observation and land subsidence observation.

References

[1] T. Schwamb, K. Soga, R. J. Mair et al., "Fibre optic monitoring of a deep circular excavation," *Proceedings of the Institution of Civil Engineers-Geotechnical Engineering*, vol. 167, no. 2, pp. 144–154, 2014.

[2] Y. C. Zheng, J. Xiong, T. Liu, X. B. Yue, and J. L. Qiu, "Performance of a deep excavation in Lanzhou strong permeable sandy gravel strata," *Arabian Journal of Geosciences*, vol. 13, no. 4, 2020.

[3] N. E. Faustin, M. Z. E. B. Elshafie, and R. J. Mair, "Case studies of circular shaft construction in London," *Proceedings of the Institution of Civil Engineers-Geotechnical Engineering*, vol. 171, no. 5, pp. 391–404, 2018.

[4] J. X. Wang, X. T. Liu, J. X. Liu, L. B. Wu, Q. F. Guo, and Q. Yang, "Dewatering of a 32.55 m deep foundation pit in MAMA under leakage risk conditions," *KSCE Journal of Civil Engineering*, vol. 22, pp. 2784–2801, 2018.

[5] J. X. Wang, X. T. Liu, Y. B. Wu et al., "Field experiment and numerical simulation of coupling non-Darcy flow caused by curtain and pumping well in foundation pit dewatering," *Journal of Hydrology*, vol. 549, pp. 277–293, 2017.

[6] Y. Tan, Y. Lu, and D. L. Wang, "Deep excavation of the Gate of the Orient in Suzhou stiff clay: composite earth-retaining systems and dewatering plans," *Journal of Geotechnical and Geoenvironmental Engineering*, vol. 144, no. 3, p. 05017009, 2018.

[7] E. Pujades and A. Jurado, "Groundwater-related aspects during the development of deep excavations below the water table: a short review," *Underground Space*, vol. 6, no. 1, pp. 35–45, 2021.

[8] J. X. Wang, B. Feng, T. P. Guo, L. G. Wu, R. X. Lou, and Z. Zhou, "Using partial penetrating wells and curtains to lower the water level of confined aquifer of gravel," *Engineering Geology*, vol. 161, pp. 16–25, 2013.

[9] Y. You, C. H. Yan, B. T. Xu, S. Liu, and C. H. Che, "Optimization of dewatering schemes for a deep foundation pit near the Yangtze River, China," *China, Journal of Rock Mechanics and Geotechnical Engineering*, vol. 10, no. 3, pp. 555–566, 2018.

[10] L. H. Liu, M. F. Lei, C. Y. Cao, and C. H. Shi, "Dewatering characteristics and inflow prediction of deep foundation pits with partial penetrating curtains in sand and gravel strata," *Water*, vol. 11, no. 10, p. 2182, 2019.

[11] L. Zhang, X. J. Zhou, Y. D. Pan, B. W. Zeng, D. F. Zhu, and H. Z. Jiang, "Design of groundwater extraction in open cut foundation pit and simplified calculation of ground subsidence due to dewatering in sandy pebble soil strata," *Advances in Civil Engineering*, vol. 2020, 25 pages, 2020.

[12] Y. Chen, W. Zhao, P. J. Jia, and J. Y. Han, "Proportion analysis of ground settlement caused by excavation and dewatering of a deep excavation in sand area," *Indian Geotechnical Journal*, vol. 48, no. 1, pp. 103–113, 2018.

[13] Y. Mei, D. Zhou, X. Wang et al., "Deformation law of the diaphragm wall during deep foundation pit construction on lake and sea soft soil in the Yangtze River Delta," *Advances in Civil Engineering*, vol. 2021, 11 pages, 2021.

[14] C. F. Zeng, X. L. Xue, G. Zheng, T. Y. Xue, and G. X. Mei, "Responses of retaining wall and surrounding ground to pre-excavation dewatering in an alternated multi-aquifer-aquitard system," *Journal of Hydrology*, vol. 559, pp. 609–626, 2018.

[15] C. F. Zeng, X. L. Xue, and M. K. Li, "Use of cross wall to restrict enclosure movement during dewatering inside a metro pit before soil excavation," *Tunnelling and Underground Space Technology*, vol. 112, p. 103909, 2021.

[16] C. Cao, C. Shi, L. Liu, and J. Liu, "Evaluation of the effectiveness of an alternative to control groundwater inflow during a deep excavation into confined aquifers," *Environmental Earth Sciences*, vol. 79, no. 22, 2020.

[17] R. Granata and F. Leoni, *In: 5th International Conference on Grouting, Deep Mixing, and Diaphragm Walls, Grouting 2017, July 9, 2017 - July 12, 2017*, American Society of Civil Engineers (ASCE), Honolulu, HI, United states, 2017.

[18] M. Calvello and R. J. Finno, "Selecting parameters to optimize in model calibration by inverse analysis," *Computers and Geotechnics*, vol. 31, no. 5, pp. 410–424, 2004.

[19] X. H. Deng, D. Y. Yuan, D. S. Yang, and C. S. Zhang, "Back analysis of geomechanical parameters of rock masses based on seepage- stress coupled analysis," *Mathematical Problems in Engineering*, vol. 2017, 13 pages, 2017.

[20] E. Pujades, A. Lopez, J. Carrera, E. Vazquez-Sune, and A. Jurado, "Barrier effect of underground structures on aquifers," *Engineering Geology*, vol. 145-146, pp. 41–49, 2012.

[21] S. L. Shen, Y. X. Wu, and A. Misra, "Calculation of head difference at two sides of a cut-off barrier during excavation dewatering," *Computers and Geotechnics*, vol. 91, pp. 192–202, 2017.

[22] H. M. Lyu, S. L. Shen, Y. X. Wu, and A. N. Zhou, "Calculation of groundwater head distribution with a close barrier during excavation dewatering in confined aquifer," *Geoscience Frontiers*, vol. 12, no. 2, pp. 791–803, 2021.

[23] J. X. Wang, X. T. Liu, J. D. Xiang, Y. H. Jiang, and B. Feng, "Laboratory model tests on water inrush in foundation pit bottom," *Environmental Earth Sciences*, vol. 75, no. 14, 2016.

[24] C. Y. Jia, H. L. Wang, H. Q. Liu, G. B. Zhang, and K. H. Sheng, "Research on the technology of plugging gushing water in the vertical shaft under complicated conditions," *Geofluids*, vol. 2020, 17 pages, 2020.

[25] X. L. Liu, F. Wang, J. Huang, S. J. Wang, Z. Z. Zhang, and K. Nawnit, "Grout diffusion in silty fine sand stratum with high groundwater level for tunnel construction," *Tunnelling and Underground Space Technology*, vol. 93, p. 103051, 2019.

[26] G. X. Zhu, Q. S. Zhang, R. T. Liu, J. W. Bai, W. Li, and X. Feng, "Experimental and numerical study on the permeation grouting diffusion mechanism considering filtration effects," *Geofluids*, vol. 2021, 11 pages, 2021.

[27] G. Zheng, C. F. Zeng, Y. Diao, and X. L. Xue, "Test and numerical research on wall deflections induced by pre-excavation dewatering," *Computers and Geotechnics*, vol. 62, pp. 244–256, 2014.